that high quality, pure, and atomically smooth *a*-axis films can be grown in situ. The single target 90° off-axis sputtering technique used maintains the surface quality over macroscopic areas and makes fabricating high T_c sandwich-type junctions possible. In fact, we have already prepared *a*-axis superlattices with $PrBa_2Cu_3O_7$ which show well-defined periods as low as 24 Å (*18, 19*). It should be possible to study transport in ribbons which are only 12 Å or less.

REFERENCES AND NOTES

1. S. W. Tozer *et al.*, *Phys. Rev. Lett.* **59**, 1768 (1987).
2. N. F. Mott, *Philos. Mag.* **22**, 7 (1970).
3. B. Oh *et al.*, *Phys. Rev. B* **37**, 7861 (1988).
4. H. Akoh, C. Camerlingo, S. Takada, *Appl. Phys. Lett.* **56**, 1487 (1990).
5. M. Lee *et al.*, in preparation.
6. K. Char *et al.*, *IEEE Trans. Magnetics* **25**, 2422 (1989).
7. C. B. Eom *et al.*, *Appl. Phys. Lett.* **55**, 595 (1989).
8. H. Asano *et al.*, *Jpn. J. App. Phys.* **28**, L981 (1989).
9. C. B. Eom *et al.*, *Physica C*, in press.
10. R. J. Cava *et al.*, *Phys. Rev. Lett.* **58**, 1676 (1987).
11. W. R. McKinnon *et al.*, *Phys. Rev. B* **38**, 6543 (1988).
12. R. J. Cava *et al.*, *Physica C* **153–155**, 560 (1988).
13. Data were taken on a Parks Scientific Instrument Model SFM-BD2 scanning force microscope.
14. J. Halbritter, *Intl. J. Mod. Phys. B* **3**, 719 (1989).
15. S. E. Russek *et al.*, *Appl. Phys. Lett.*, in press.
16. C. P. Bean, *Phys. Rev. Lett.* **54**, 1702 (1962).
17. D. Dimos, P. Chaudhari, J. Mannhart, F. K. LeGoues, *Phys. Rev. Lett.* **61**, 219 (1988).
18. C. B. Eom and T. H. Geballe, paper presented at 1990 MRS Spring Meeting (San Francisco, 20 April 1990), Symposium M.
19. C. B. Eom *et al.*, in preparation.

20. We thank M. D. Kirk and R. S. Howland for the SFM image of the *a*-axis film surface and J. Halbritter for helpful discussions. This work has been supported by AFOSR under contract F49620-88-C-004, by the Center for Research in Superconductivity and Superconducting Electronics under contract F49620-88-C-001 and by the Stanford Center for Materials Research under the NSFMRL program.

20 July 1990; accepted 14 August 1990

Direct Interaction of a Ligand for the *erb*B2 Oncogene Product with the EGF Receptor and p185^{erbB2}

RUTH LUPU,* RAMON COLOMER, GERHARD ZUGMAIER, JAY SARUP, MICHAEL SHEPARD, DENNIS SLAMON, MARC E. LIPPMAN

The *erb*B2 oncogene encodes a 185-kilodalton transmembrane protein whose sequence is similar to the epidermal growth factor receptor (EGFR). A 30-kilodalton factor (gp30) secreted from MDA-MB-231 human breast cancer cells was shown to be a ligand for p185^{erbB2}. An antibody to EGFR abolished the tyrosine phosphorylation induced by EGF and transforming growth factor–α (TGF-α) but only partially blocked that produced by gp30 in SK-BR-3 breast cancer cells. In two cell lines that overexpress *erb*B2 but do not express EGFR (MDA-MB-453 breast cancer cells and a Chinese hamster ovary cell line that had been transfected with *erb*B2), phosphorylation of p185^{erbB2} was induced only by gp30. The gp30 specifically inhibited the growth of cells that overexpressed p185^{erbB2}. An antibody to EGFR had no effect on the inhibition of SK-BR-3 cell colony formation obtained with gp30. Thus, it appeared that gp30 interacted directly with the EGFR and *erb*B2. Direct binding of gp30 to p185^{erbB2} was confirmed by binding competition experiments, where gp30 was found to displace the p185^{erbB2} binding of a specific antibody to p185^{erbB2}. The evidence described here suggests that gp30 is a ligand for p185^{erbB2}.

THE HUMAN C-*erb*B2 ONCOGENE encodes a 185-kD transmembrane glycoprotein with tyrosine kinase activity. This protein, p185^{erbB2}, shows extensive structural similarity with the p170 EGFR and is thought to be a growth factor receptor (*1–4*). No ligand for p185^{erbB2} has as yet been fully characterized. EGF and TGF-α, the normal ligands for the EGFR, do not interact directly with p185^{erbB2} (*5, 6*). Amplification of *erb*B2 occurs in many adenocarcinomas and it is overexpressed in nearly 30% of human breast cancer patients (*7–9*). In addition, p185^{erbB2} is necessary for the maintenance of the malignant phenotype of cells transformed by *erb*B2 (*10*).

We have previously identified and purified a growth factor that is secreted by MDA-MB-231 human breast cancer cells (*11*). This 30-kD glycoprotein (gp30) is similar to TGF-α in its ability to bind to the EGFR, phosphorylate EGFR, and induce NRK colony formation. However, it is distinct from the 18-kD precursor for TGF-α and 6-kD mature TGF-α, as shown by peptide mapping of the translated proteins (*11*). The purification profile of the preparation of the 30-kD polypeptide used in the current studies is shown in Fig. 1.

To characterize the cellular effects of gp30, we assessed its ability to induce tyrosine phosphorylation in human breast cancer cell lines MDA-MB-468 and SK-BR-3. The *EGFR* gene is amplified and overexpressed in MDA-MB-468 cells (*7*), although they do not express detectable concentrations of *erb*B2. Amplification and overexpression of the *erb*B2 gene occur in SK-BR-3 cells, and they also have moderately elevated concentrations of the EGFR (*12*). TGF-α, gp30 (Fig. 2), and EGF induced tyrosine phosphorylation in both cell lines. An antibody against the EGFR (anti-EGFR) abolished the phosphorylation induced by the three growth factors in MDA-MB-468 cells. However, this antibody did not completely block the phosphorylation induced by gp30 in SK-BR-3 cells, although in these cells it blocked the phosphorylation induced by TGF-α (Fig. 2). This result suggested that tyrosine phosphorylation of a protein different from the EGFR occurred in gp30-treated SK-BR-3 cells. No phosphorylation was observed in untreated SK-BR-3 cells or cells treated only with the antibody to EGFR (Fig. 2).

To test whether this tyrosine phosphorylated protein was p185^{erbB2}, we used the human mammary carcinoma cell line MDA-MB-453 (*12*), which overexpresses *erb*B2 but has undetectable concentrations of the EGF receptor protein or mRNA (*13*). In these cells, gp30 induced a significant increase in tyrosine phosphorylation in a dose-dependent manner (Fig. 3).

To further analyze the effects of gp30, we studied Chinese hamster ovary (CHO) cells transfected with human *erb*B2 (CHO/*erb*B2) (*14, 15*). Induction of p185^{erbB2} phosphorylation was detected in gp30-treated CHO/*erb*B2 cells with an antibody to phosphotyrosine (Fig. 4). No tyrosine phosphorylation was observed in control CHO cells transfected with the gene for dihydrofolate reductase (DHFR) (CHO/DHFR) or in untreated cells. Levels of p185^{erbB2} did not change after treatment with gp30 in CHO/*erb*B2 cells (Fig. 4).

In summary, in all the cell lines described above, EGF and TGF-α were unable to induce p185^{erbB2} phosphorylation. No phosphorylation was observed in untreated cells. This supported the hypothesis of an apparently direct interaction between gp30 and p185^{erbB2}

We next examined the effects of gp30 on

R. Lupu, R. Colomer, G. Zugmaier, M. E. Lippman, The Vincent T. Lombardi Cancer Research Center, Georgetown University Medical Center, 3800 Reservoir Road, Washington, DC 20007.
J. Sarup and M. Shepard, Genentech, San Francisco, CA 94080.
D. Slamon, Division of Hematology-Oncology, Department of Medicine, UCLA, Los Angeles, CA 90024.

*To whom correspondence should be addressed.

the proliferation and colony formation of breast carcinoma cell lines. Cells were treated with gp30, EGF, TGF-α, and a specific monoclonal antibody (MAb) to *erb*B2, which binds to p185^{erbB2} and inhibits the growth of cells with *erb*B2 amplification (*16*). Exposure of SK-BR-3, MDA-MB-453, and MDA-MB-468 cells to gp30 produced a 60 to 70% inhibition of their cell growth, and the growth of CHO/*erb*B2 cells was inhibited by 70 to 80%. Treatment with gp30 had no effect on the cell growth of the cell lines with low amounts of p185^{erbB2} (Table 1). The antibody (4D5) inhibited the proliferation of the SK-BR-3, MDA-MB-453, and CHO/*erb*B2 cells by 60 to 70%, but did not inhibit the proliferation of MDA-MB-468 cells.

Furthermore, inhibition of growth by gp30 was reversed by anti-EGFR in MDA-MB-468 cells, but not in SK-BR-3 or MDA-MB-453 cells, again indicating that the effects of gp30 on SK-BR-3 and MDA-MB-453 cells were not mediated through the EGFR. This growth-inhibitory property of gp30 seems similar to that described for EGF on cells that overexpress EGFR, such

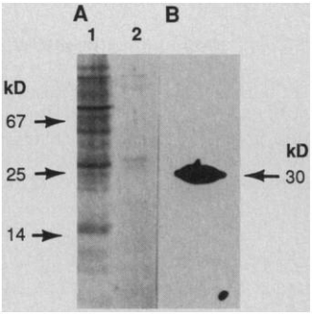

Fig. 1. Isolation of gp30. (**A**) Low-affinity heparin chromatography. Affinity chromatography of conditioned media from MDA-MB-231 cells was performed on a heparin-Sepharose column. Fractions were analyzed for EGFR binding activity on A431 cell membranes (*11*). Aliquots from the input media and from the fractions containing activity were analyzed by a 15% SDS-PAGE (*25*), followed by silver staining (*26*). Lane 1 shows unconcentrated conditioned media. Lane 2 represents the active fraction. (**B**) Reversed-phase chromatography. The EGF/TGF-α active fractions obtained after heparin-Sepharose chromatograph were chromatographed twice on a μBondapak C_3 column in 0.05% trifluoroacetic acid. Samples were eluted with a steep gradient of acetonitrile. Fractions that showed EGFR binding activity were then rechromatographed and eluted with a shallow acetonitrile gradient. EGF competing activity was constantly eluted at a 25 to 30% acetonitrile gradient. The resulting fraction was analyzed on a 15% SDS-PAGE followed by silver staining.

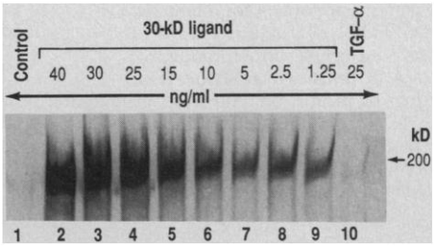

Fig. 3. Detection of phosphorylated proteins in MDA-MB-453 cells. MDA-MB-453 cells were grown to 90% confluence in 24-well plates (Costar) and treated at 37°C with IMEM (lane 1), IMEM containing recombinant TGF-α (25 ng/ml) (Genentech) (lane 10), or IMEM containing gp30 (1.25 to 40 ng/ml) (lanes 2 to 9). After 20 min, media was removed and cells were lysed in 100 μl of sample buffer as described in Fig. 2. After 5 min at 95°C, 50 μg of protein was loaded in a 7.5% SDS-PAGE. Proteins were then transferred to nitrocellulose membrane for immunoblotting with an antibody to phosphotyrosine (Amersham) as described in Fig. 2.

Table 1. Cell growth inhibition induced by gp30. SK-BR-3, MDA-MB-453, MDA-MB-468, and MCF7 cells were plated in 24-well plates in IMEM (Biofluids) supplemented with 5% fetal calf serum (FCS). Parental CHO cells, and CHO cells transfected with the *DHFR* gene or the *erb*B2 gene were plated in 24-well plates (Costar) in α-MEM (Biofluids) supplemented by 10% dialyzed FBS, G418 (0.75 mg/ml), and methotrexate (MTX) 50 nM for the CHO parental and CHO/DHFR cells or 250 nM for the CHO/*erb*B2 cells. After 24 hours, media was removed and replaced with control serum-free media (SFM) containing fibronectin, transferrin, Hepes, glutamine, trace elements, and BSA or SFM with the addition of gp30 (2.0 ng/ml), recombinant TGF-α (10 ng/ml) (Genentech), or with 4D5 specific anti-p185^{erbB2} MAb (2.5 μg/ml). Cells were grown to 90% confluence of control and counted. Each group was assayed in triplicate. Results (mean ± SD) are shown as growth relative to control. The experiments were performed three times and the results were reproducible.

	SK-BR-3	MDA-MB-453	CHO/*erb*B2	CHO/DHFR	MDA-MB-468	MCF7
gp30	31	24	20	99	18	100
4D5 antibody	32	34	22	98	104	92
TGF-α	73	91	89	95	79	105
Control antibody	87	91	87	94	92	99

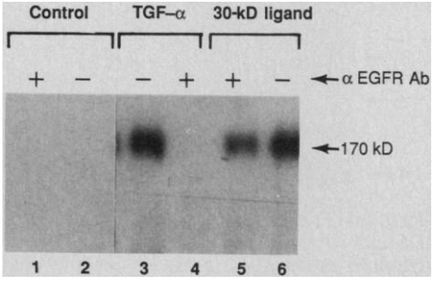

Fig. 2. Detection of phosphorylated proteins in SK-BR-3 cells. SK-BR-3 cells were grown to 90% confluence in 24-well plates (Costar). Cells were treated at 37°C with IMEM (lanes 1 and 2), IMEM containing recombinant TGF-α (25 ng/ml; Genentech) (lanes 3 and 4), and IMEM containing gp30 (5 ng/ml) (lanes 5 and 6), in the presence (lanes 1, 4, and 5) or absence (lanes 2, 3, and 6) of an anti-EGFR (Genentech). After 20 min, the media was removed and cells were lysed in 100 μl of sample buffer containing 1% SDS, 0.1% β-mercaptoethanol, 0.15 M tris-HCl (pH 6.8), 10% glycerol, 0.02% bromophenol blue, 1 mM EDTA, 2 mM phenylmethylsulfonyl fluoride (PMSF), and 42 mM leupeptin. After 5 min at 95°C, 50 μg of protein were loaded in a 7.5% SDS-PAGE. Proteins were then transferred to nitrocellulose membrane for immunoblotting (Hoefer Scientific Instruments) by electrophoresis in a modified method of Towbin *et al.* (*27*) with an electrophoretic transfer unit (Hoefer, TE 22). Electrophoretic transfer was carried out at room temperature for 1 hour at 125 mA in a buffer containing 25 mM glycine, 129 mM tris (pH 8.3), and 20% methanol. After transfer, the filter was blocked with 5% bovine serum albumin (BSA) in tris-buffered saline containing 0.5% Tween 20. An antibody to phosphotyrosine (Amersham) was reacted with the immobilized proteins in 5% BSA (Sigma RIA grade). Immune complexes were detected by a goat antibody to mouse conjugated to alkaline phosphatase. Blots were then incubated with a color development substrate solution containing nitroblue tetrazolium and 5-bromo-4-chloro-3-indolyl phosphate (Promega).

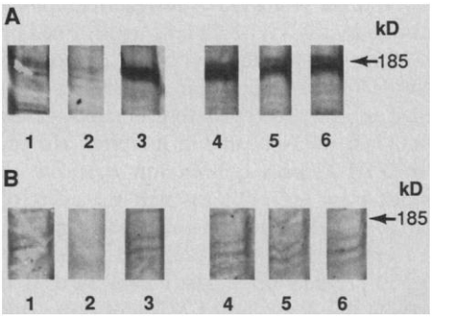

Fig. 4. Phosphorylation of p185^{erbB2} protein in intact CHO/DHFR, and CHO/*erb*B2 cells. Cells were grown to 90% confluence in 24-well plates (Costar) in α-MEM (Biofluids) supplemented with 10% dialyzed FCS, G418 (0.75 mg/ml), and methotrexate (MTX) at concentrations of 50 nM (CHO parental and CHO/DHFR) or 250 nM (CHO/*erb*B2). CHO/DHFR (Fig. 4A) and CHO/*erb*B2 (Fig. 4B) cells were treated at 37°C with control media supplemented with 20 mM Hepes (pH 7.4) [(A) and (B), lanes 1 and 4], with recombinant TGF-α (10 ng/ml) (Genentech) [(A) and (B), lanes 2 and 5], and control media supplemented with gp30 (2.0 ng/ml) [(A) and (B), lanes 3 and 6]. After 20 min, media was removed and cells were lysed in 100 μl of sample buffer (as described in Fig. 2). An antibody to phosphotyrosine [(A) and (B), lanes 1 to 3] (Amersham) and an antibody to *erb*B2 [(A) and (B), lanes 4 to 6] (NEN) were reacted with the immobilized proteins in 5% BSA (Sigma RIA grade). Immunocomplexes were detected as described in Fig. 2.

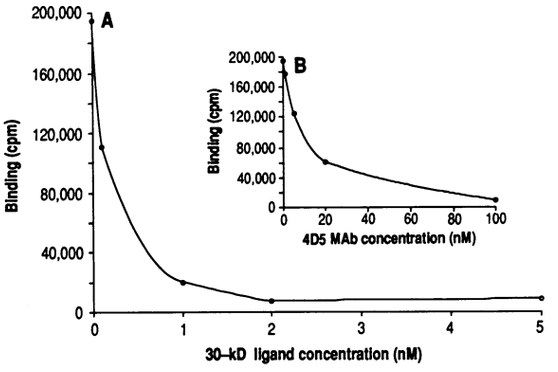

Fig. 5. p185^{erbB2} receptor competition assay in SK-BR-3 cells. SK-BR-3 cells were plated in 24-well plates in IMEM (Biofluids) supplemented with 5% FCS. After washing with binding buffer [DMEM-F12, pH 7.4, containing BSA (1 mg/ml), Hepes (10 mM), and glutamine (20 mM)], we incubated cells for 30 min at 37°C with binding buffer. The EGFR were saturated with 30 nM EGF for 2 hours at 4°C. p185^{erbB2} binding studies were then performed for 3 hours at 4°C with 1 nM iodinated 4D5 in the presence of various concentrations of unlabeled gp30 or 4D5. After the incubation, cells were washed three times with binding buffer and then solubilized with 1% SDS. No specific binding was determined with excess (100 nM) of unlabeled antibody. Each group was assayed in triplicate. The experiments were performed five times and the results were reproducible. (**A**) Competition of the binding of iodinated 4D5 MAb to the *erb*B2 receptor by the 30-kD ligand. (**B**) Competition of the binding of iodinated 4D5 MAb to the *erb*B2 receptor by 4D5 MAb.

as A431 cells (*4, 17*) and MDA-MB-468 cells (*18*). In separate experiments, gp30, EGF, and TGF-α were shown to induce cell proliferation of NRK cells and immortalized human breast epithelial A1N4 cells. Therefore, all three ligands have stimulatory activity in cells containing normal amounts of EGFR, probably because of their ability to interact with EGFR. Perhaps gp30 hyperstimulates cells that express very high amounts of *erb*B2 or EGFR, analogous to the action of EGF in cells that overexpress EGFR.

Hudziak *et al.* (*16*) showed that colony formation of NIH-3T3 cells transformed by *erb*B2 could be inhibited by an antibody to anti-*erb*B2. Drebin *et al.* (*19–20*) reported that an anti-p185^{neu} MAb generated against mutated rat Neu protein inhibited growth of NIH-3T3/*neu* cells in soft agar and in nude mice (*21*). We assessed the effect of gp30 on the anchorage-independent growth of breast cancer cells (*22*) and found that gp30 prevented soft agar colony formation of SK-BR-3 and MDA-MB-453 cells. This inhibition was not reversed by an antibody to the EGFR in SK-BR-3 cells. Treatment of SK-BR-3 cells with 4D5 (anti-*erb*B2) reduced their ability to form colonies in soft agar.

To determine whether gp30 binds specifically to p185^{erbB2}, we performed p185^{erbB2} binding competition assays. Since iodinated gp30 was not available, we used an iodinated anti-*erb*B2 (4D5) that induced similar biological responses to gp30 in cells with *erb*B2 overexpression. We hypothesized that the antagonistic effects were exerted near the ligand binding site in p185^{erbB2}, and therefore that gp30 and 4D5 would compete with each other for binding to the receptor. Iodinated 4D5 MAb was used for the receptor binding experiments, in the presence of increasing concentrations of gp30. The gp30 displaced 4D5 binding to p185^{erbB2} in intact SK-BR-3 and MDA-MB-453 cells (Fig. 5), implying that gp30 binds to the receptor. The binding of a control iodinated antibody to *erb*B2 that does not show antiproliferative effects (6E9) was not altered by gp30. The gp30 binding activity was not inhibited by excess concentrations of EGF or TGF-α.

To verify that the receptor competition was specific, we covalently cross-linked iodinated 4D5 to p185^{erbB2} in the presence of gp30. The complex was immunoprecipitated with an antibody to the COOH-terminal domain of p185^{erbB2} (*23*) and analyzed by SDS–polyacrylamide gel electrophoresis (PAGE). The autoradiogram showed a specific high molecular weight 4D5 binding site. Cross-linking of p185^{erbB2} and iodinated 4D5 was blocked in the presence of gp30, but blocking was not observed in the presence of EGF (Fig. 6).

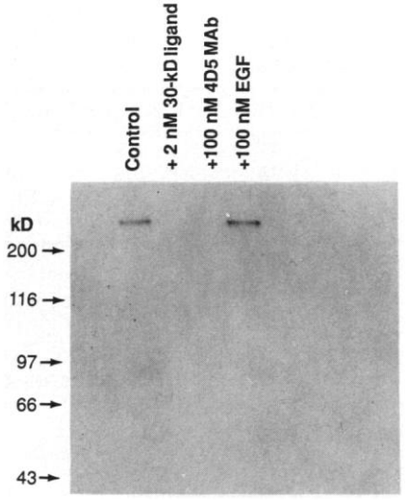

Fig. 6. Inhibition of p185^{erbB2} cross-linking with 4D5 antibody by gp30. The binding assays were performed as described in Fig. 5. Binding was performed with iodinated 4D5 (1 nM) alone (lane 1), in the presence of 100 nM unlabeled 4D5 (lane 2), and in the presence of 2 nM gp30 (lane 3). EGF (100 nM) was used as a control (lane 4). Cells were then treated with a cross-linking agent (ethylene glycol succinate) for 45 min at 4°C and then quenched by adding 0.1 ml of 20 mM NH_4Cl. The solubilized cells were immunoprecipitated with a polyclonal antibody to the COOH-terminal domain of *erb*B2 (Genentech). The precipitates were analyzed on a 5% SDS-PAGE.

In summary, our findings suggest that gp30 secreted by the MDA-MB-231 breast cancer cell line is a ligand for p185^{erbB2}. The ability of gp30 to induce NRK cell proliferation and soft agar colony formation indicates that it has growth factor–stimulatory abilities, and it was also able to stimulate p185^{erbB2} and EGFR phosphorylation. Therefore, gp30 seems to interact directly and independently with p185^{erbB2} and EGFR. This observation is distinct from the described tyrosine kinase phosphorylation of p185^{erbB2} that is induced after activation of EGFR (*7–9*).

The gp30 inhibited growth of cells overexpressing *erb*B2 or EGFR instead of stimulating their growth. Whether this polypeptide is a true inhibitory factor or produces inhibition by an autocrine hyperstimulation similar to that observed with EGF in cells overexpressing the EGFR (*18*) remains unsolved. Metabolic labeling and immunoprecipitation analysis of SK-BR-3 cells suggests that they secrete low concentrations of gp30. Additional data show that low amounts of exogenous gp30 slightly stimulate rather than inhibit the growth of SK-BR-3 cells (*24*), which would favor the autocrine hypothesis. The mechanism by which 4D5 affects the growth of cells overexpressing *erb*B2 is presently unclear. Hudziak *et al.* showed that 4D5 down-regulated p185^{erbB2} in SK-BR-3 cells (*16*) and suggested that it might interfere with the binding of p185^{erbB2} to its ligand. The competition assays and the ability of gp30 to block the cross-linking of 4D5 to its receptor demonstrated that gp30 and 4D5 compete for p185^{erbB2} binding. We therefore conclude that gp30 is a ligand for *erb*B2. However, the growth stimulation of SK-BR-3 cells observed with low concentrations of gp30 was not blocked by the antibody (*24*). Further analysis will be needed to understand the role of the *erb*B2 gene product and its ligand in normal and malignant cell growth and development.

REFERENCES AND NOTES

1. Y. Yarden *et al.*, *EMBO J.* **6**, 3341 (1987).
2. C. I. Bargmann and R. A. Weinberg, *ibid.* **7**, 2043 (1988).
3. E. J. J. van Zoelen, M. A. van Rooijen, T. M. J. van Oostwaard, S. W. de Laat, *Cancer Res.* **47**, 1582 (1987).

4. T. Kawamoto *et al.*, *Proc. Natl. Acad. Sci. U.S.A.* **80**, 1337 (1983).
5. C. R. King *et al.*, *EMBO J.* **7**, 1647 (1988).
6. D. F. Stern and M. P. Kamps, *ibid.*, p. 995.
7. M. H. Kraus *et al.*, *ibid.* **6**, 605 (1987).
8. D. J. Slamon *et al.*, *Science* **235**, 177 (1987).
9. M. Van de Vijver *et al.*, *Mol. Cell. Biol.* **7**, 2019 (1987).
10. D. Slamon *et al.*, *Science* **244**, 707 (1989).
11. R. Lupu *et al.*, in preparation.
12. SK-BR-3, MDA-MB-453, and MDA-MB-468 cells were obtained from American Type Culture Collection (ATCC, Rockville, MD). MCF7 cells were originally obtained from M. Rich, Michigan Cancer Foundation. CHO cells were from L. Chesin. Media used for routine growth and plating of each cell line are described in the text. SK-BR-3, MDA-MB-453, and CHO/*erb*B2 cells express high amounts of $p185^{erbB2}$. MDA-MB-468 cells express high amounts of EGFR, and SK-BR-3 expresses intermediate amounts of EGFR. MDA-MB-468, MCF7, CHO, and CHO/DHFR cells express low or undetectable amounts of $p185^{erbB2}$. MDA-MB-453, MCF7, CHO, CHO/DHFR, and CHO/*erb*B2 cells express low or undetectable amounts of EGFR. $p185^{erbB2}$ and EGFR concentrations were determined by immunoblotting.
13. Y. Yarden and R. A. Weinberg, *Proc. Natl. Acad. Sci. U.S.A.* **86**, 3179 (1989).
14. C. Chen and H. Okayama, *Mol. Cell. Biol.* **8**, 2745 (1987).
15. The CHO/*erb*B2 cell line was prepared by V. Campbell, University of California, Los Angeles, by the following method. The c-*erb*B2 gene was cloned from a primary human breast carcinoma tissue specimen and characterized [D. Slamon *et al.*, *Cancer Cells* 7, 371 (1989)]. The gene was cloned into a cytomegalovirus (CMV)-based expression vector that also contained selectable markers for neomycin resistance and a functional dihydrofolate reductase gene. Chinese hamster ovary cells received from L. Chasin [G. Urlaub and L. Chasin, *Proc. Natl. Acad. Sci. U.S.A.* 77, 4216 (1980)] were transfected (*20*) with the c-*erb*B2/CMV expression vector. Two days after transfection the cells were split 1:7 and placed into selective media [α-minimum essential medium (MEM) without nucleosides containing 50 nM methotrexate (MTX), G418 (0.75 mg/ml), and 10% dialyzed fetal bovine serum (FBS)]. After 2 weeks of growth in selective media, the resulting colonies were cloned with glass cloning cylinders. Cells were trypsinized and transferred into 24-well plates. Cells were screened for c-*erb*B2 expression by immunohistochemistry and immunoblot analysis. Positive colonies were amplified for content of the c-*erb*B2 gene by sequentially increasing the concentration of methotrexate in the growth media up to a final concentration of 500 nM.
16. R. M. Hudziak *et al.*, *Mol. Cell. Biol.* **9**, 1165 (1989).
17. T. Kawamoto *et al.*, *J. Biol. Chem.* **259**, 7761 (1984).
18. B. W. Ennis *et al.*, *Mol. Endocrinol.* **3**, 1830 (1989).
19. J. A. Drebin *et al.*, *Oncogene* **2**, 387 (1988).
20. ———, *ibid.*, p. 273.
21. J. A. Drebin *et al.*, *Proc. Natl. Acad. Sci. U.S.A.* **83**, 9129 (1986).
22. Soft agar colony formation assays were performed as follows. In 35-mm tissue culture dishes (Costar, Cambridge, MA), a bottom layer of 1.0 ml of improved MEM (IMEM) containing 0.6% agar and 10% FBS was prepared. After the bottom layer was solidified, the indicator cells (10,000 per dish) were added in a top layer (0.8 ml) containing the sample, 0.4% Bacto Agar (Difco), and 10% FBS. The samples were gp30 (2.0 ng/ml) and EGF (10 ng/ml), in the presence or absence of an anti-EGF receptor (1.25 μg/ml) or an anti-*erb*B2 MAb 4D5 (2.5 μg/ml). A nonspecific MAb (354) served as control. All samples were run in triplicates, and experiments were carried out in FBS that had been tested for optimal cloning efficiency. Cells were incubated 7 to 9 days at 37°C in 5% CO_2 atmosphere. Colonies larger than 60 μm were counted in a cell colony counter. Experiments were performed three times, and the results were reproducible.
23. B. M. Fendly *et al.*, *Cancer Res.* **50**, 1550 (1990).
24. R. Lupu *et al.*, unpublished data.
25. U. K. Laemmli, *Nature* **227**, 680 (1970).
26. J. H. Morissey, *Anal. Biochem.* **177**, 307 (1981).
27. H. Towbin, T. Staehelin, J. Gordon, *Proc. Natl. Acad. Sci. U.S.A.* **76**, 4350 (1979).
28. We thank F. Kern for critical review and comments on the manuscript, and R. B. Dickson, R. King, K. Cullen, and E. Thompson for their helpful discussions.

6 February 1990; accepted 28 June 1990

Retroviral DNA Integration Directed by HIV Integration Protein in Vitro

FREDERIC D. BUSHMAN,* TAMIO FUJIWARA,† ROBERT CRAIGIE

Efficient retroviral growth requires integration of a DNA copy of the viral RNA genome into a chromosome of the host. As a first step in analyzing the mechanism of integration of human immunodeficiency virus (HIV) DNA, a cell-free system was established that models the integration reaction. The in vitro system depends on the HIV integration (IN) protein, which was partially purified from insect cells engineered to express IN protein in large quantities. Integration was detected in a biological assay that scores the insertion of a linear DNA containing HIV terminal sequences into a λ DNA target. Some integration products generated in this assay contained five–base pair duplications of the target DNA at the recombination junctions, a characteristic of HIV integration in vivo; the remaining products contained aberrant junctional sequences that may have been produced in a variation of the normal reaction. These results indicate that HIV IN protein is the only viral protein required to insert model HIV DNA sequences into a target DNA in vitro.

RETROVIRUSES ENCODE A PROTEIN, IN protein, that is necessary for normal integration of retroviral DNA and efficient retroviral growth (*1, 2*). Studies of several retroviruses suggest that integration involves a coordinated set of DNA cleaving and joining reactions mediated by IN protein. First, the flush-ended linear DNA produced by reverse transcription is prepared for integration by IN protein–dependent cleavage, yielding recessed 3′ ends. In the Moloney murine leukemia virus (M-MuLV) system, production of these recessed ends in vivo depends on the viral IN function (*3, 4*); purified avian myeloblastosis virus (AMV) IN protein can carry out this reaction in vitro (*5*). Next, viral DNA is inserted into a DNA target, a reaction that also has been shown to depend on IN function in several retroviral systems in vivo (*2*). Analysis of a DNA intermediate of M-MuLV integration indicates that the recessed 3′ ends of the viral DNA are joined to the 5′ ends of a double-strand break made in the DNA target (*3, 6*); staggered cleavage of the target DNA is inferred from the short duplication of target DNA that flanks the integrated proviral DNA. Integration is completed by removal of unpaired bases at the 5′ ends of the viral DNA and repair of the resulting single-stranded gaps, presumably by cellular DNA repair enzymes, yielding the short duplication of the target DNA at the point of insertion. Each retroviral integration system generates a target duplication of characteristic length, ranging from 4 to 6 bp (*1*).

The human immunodeficiency virus (HIV) genome encodes an IN protein that is similar in sequence to those of other retroviruses (*7*), and the HIV integration function is known to be required in vivo for

Laboratory of Molecular Biology, National Institute of Diabetes, and Digestive and Kidney Diseases, National Institutes of Health, Bethesda, MD 20892.

*To whom correspondence should be addressed.
†Present and permanent address: Shionogi Institute for Medical Science, Osaka 566, Japan.

Table 1. Integration of mini-HIV in the presence of partially purified HIV IN protein. Line 1 presents the results of 21 independent reactions; line 2 presents the results of 6 independent reactions. Integration reactions contained 10 μl of partially purified HIV IN protein or the same volume of the corresponding protein preparation made from uninfected cells, 1 μg of mini-HIV DNA, 1.5 μg of λ DNA, bovine serum albumin (0.1 mg/ml) RNase A (0.1 mg/ml), RNase T1 (2 U/ml), *Xenopus* histone H1 (20 μg/ml), protein HU (2 μg/ml) (*22*), 130 mM potassium glutamate, 20 mM Hepes (pH 7.5), 5 mM $MgAc_2$, 10 mM dithiothreitol, 0.05% NP-40, 10% dimethyl sulfoxide, and 10% glycerol in a final volume of 50 μl. Reaction mixtures were incubated at 0°C for 1 hour, then 8 μl of 30% polyethylene glycol was added, and the reactions were incubated for 30 min at 30°C.

Integration protein	Colonies	Phage
HIV IN	71	5.9×10^9
Control insect cell extract	0	1.3×10^9